X-ray Structure Analysis of an Aromatic Polyimide

Yutaka Obata, Kenji Okuyama,* and Sonoko Kurihara

Faculty of Technology, Tokyo University of Agriculture and Technology, Koganei, Tokyo 184, Japan

Yukishige Kitano

Toray Research Center, Inc., Sonoyama, Otsu, Shiga 520, Japan

Takuma Jinda

Kyushu Women's Junior College, Yahatanishi, Kitakyushu, Fukuoka 807, Japan

Received May 19, 1994; Revised Manuscript Received November 15, 1994®

ABSTRACT: The molecular conformation and crystal structure of an aromatic polyimide, poly[(4,4'-diphenylene)pyromellitimide] (PMB), was analyzed by means of X-ray diffraction and a linked-atom least-squares method. X-ray diffraction intensity data were recorded on an imaging plate and measured by the newly developed intensity measuring system. The unit cell was orthorhombic and its dimensions were $a = 8.57$, $b = 5.51$, and c (fiber axis) $= 16.78$ Å. The space group symmetry was *Pbam*. There were two parallel 1/1 helical chains in a unit cell, one at the corner and the other at the center. The corner and the center one were related by the glide symmetry parallel to the a- and b-axis. Two benzene rings in the biphenyl moiety had a coplanar conformation. The extended polymer chains were aligned along the c-axis in which the pyromellitimide plane and the biphenyl plane were inclined +57° and −58° to the (010) plane, respectively. Because of the glide symmetry, two adjacent pyromellitimide groups were aligned side by side with the same height along the c-axis. The molecular conformations were stabilized only by van der Waals interactions.

Introduction

The polyimide is an excellent thermostable and a low thermal expansive aromatic polymer. It has good mechanical properties and a low dielectric constant. Due to its superior physical properties, such as insulation resistance and mechanical strength at high temperature, polyimide has been widely used as industrial materials such as parts of aircraft, machines, and electronic appliances. In order to understand its physical properties, it is important to get the precise structural information. Since polyimides synthesized so far have had poor crystallinity, X-ray diffraction data were not sufficient to give the precise structure. Therefore, only a few structures have been analyzed.[1,2] It was found that the typical texture of polyimide was mesomorphic or amorphous. To obtain the oriented crystalline texture was very difficult as well.[3] However, the rigid-rod type polyimide may crystallize easily during the thermal imidization and have a high crystallinity. Since all rotating bonds are aligned in the same direction and the repeating unit distance of each orientation is the same, the number of parameters to define the packing structure is small. The structure analysis was not too difficult to be analyzed by the X-ray diffraction technique.

In this paper, the molecular and crystal structures of a rigid-rod type polyimide; i.e., poly[(4,4'-diphenylene)pyromellitimide] (PMB), were analyzed by using a linked-atom least-squares method together with X-ray diffraction data. X-ray diffraction intensities were collected by the new system of intensity measurement[4] combined with an imaging plate instead of the conventional X-ray film method.

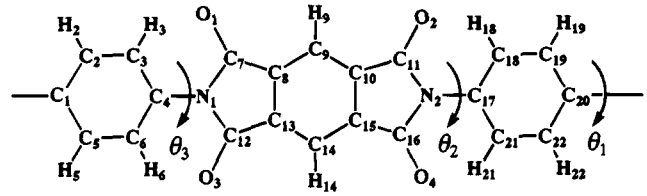

(a)

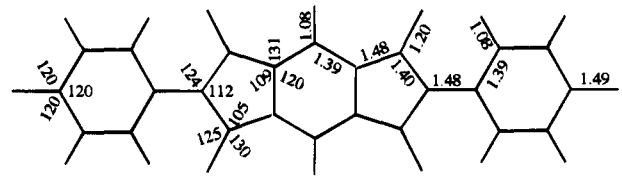

(b)

Figure 1. (a) Chemical structure of a repeating unit of PMB and dihedral angles varied in the refinement. (b) Bond lengths (Å) and angles (deg) used in the molecular model building.

Materials and Methods

Preparation of Specimens. The material used for polyimide could be prepared through poly(amic acid) transition. Poly(amic acid) was synthesized from pyromellitic dianhydride and aromatic diamines in a *n*-methyl-2-pyrrolidone (NMP) solution. After these poly(amic acid)s were cooled under ice water, the mixture of acetic anhydride and pyridine in NMP solution to become the polyimide (PMB) was added dropwise so as to imidize the poly(amic acid). The wet-spun fibers of PMB were obtained by extruding the polymer solution from a capillary spinneret into the coagulation bath containing the mixture of NMP and water. This fiber was drawn up to 1.5 times of the original length in water at room temperature. And then the fiber was heated in an oven at 575 °C. The density of the specimen was measured by a flotation method using a mixture of *n*-heptane and carbon tetrachloride. The measurement was carried out at 25 °C. Details of the specimen preparation are given elsewhere.[5]

* Corresponding author.

® Abstract published in *Advance ACS Abstracts,* January 15, 1995.

0024-9297/95/2228-1547$09.00/0

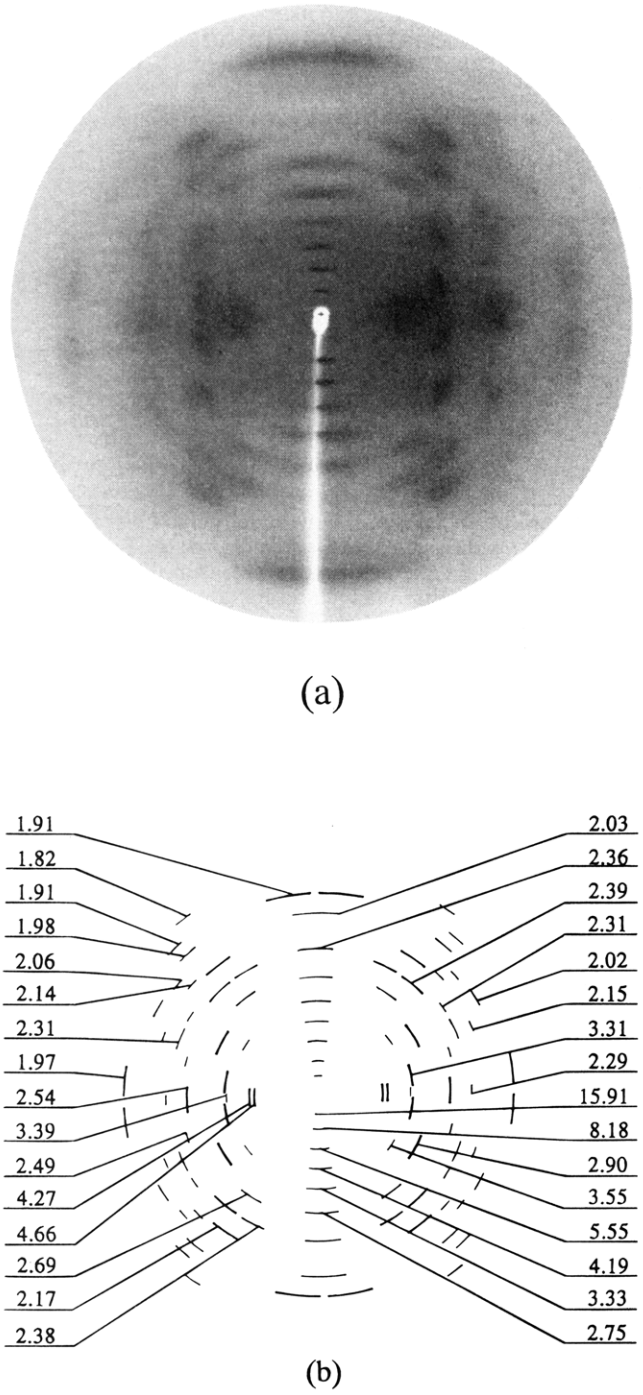

Figure 2. (a) X-ray diffraction diagram of PMB taken by an imaging plate. This pattern is a hard copy from the display. (b) Its schematic illustration with measured spacings in angstroms.

X-ray Diffraction Measurement. The X-ray diffraction diagram was recorded by a camera system[6] connected with an imaging plate (DIP-100S, MAC Science Co. Ltd.). The system used graphite monochromatized Cu Kα radiation (1.5418 Å) from an X-ray generator (Rotaflex RU-200, Rigaku Co. Ltd.) with a rotating anode. The DIP-100S was driven directly by a VME (Versa Module Europe) crate controlled by a Motorola 68000 processor. This processor was connected to a graphics workstation (SPARCstation 2, Sun Microsystems Computer Co. Ltd.). The imaging plate covered with a photostimulable phosphor ($BaFBr:Eu^{2+}$, 0.15 mm in thickness)[7] was used to record X-ray diffraction diagrams. The size of the imaging plate is 20 cm diameter. Since the pixel size was designed to be 0.125 × 0.125 mm^2, a total of 1600 × 1600 pixels were sufficient to cover a whole area of the imaging plate. The diffraction pattern was then read by measuring the fluorescence intensity stimulated by a focused He–Ne laser beam (633 nm) scanning on the surface of the imaging plate. The intensity of each pixel was expressed in 2 byte. To store pixel data in each frame of the imaging plate, 5.12 MB was required. The Bragg spacing was obtained by averaging the distances between the center of the diffraction diagram and positions of two or four equivalent reflections. The unit cell dimensions were determined by the least-squares method with the given initial cell dimensions. The removal of background intensity was carried out at each diffraction spot. The background intensity was estimated from the volume under the surface defined by the average value of the five lowest intensities in the four subareas around the diffraction spot. We assumed the shape of the diffraction spot to be an ellipse, which was defined by the width along the radial direction and the azimuthal angle from the center of the diffraction diagram. The intensity (I_o) was determined by integrating the intensity of each pixel within this ellipse. Overlapped reflections were resolved using a Gaussian approximation.[4]

Table 1. Final Parameters of Four Molecular Models of PMB

	model A	model A′	model B	model B′
space group	$P2_12_12$	$P2_12_12$	$P2_12_12$	*Pbam*
dihedral angles/deg				
θ_1	20.7	159.2	0.4	(0.0)
θ_2	−75.9	76.0	−65.6	−65.0
θ_3[a]	(55.2)	(124.9)	(65.2)	(65.0)
μ	56.4	56.4	56.5	56.6
w	0.296	0.296	0.301	(0.298)
scale factor	4.71	4.71	4.75	4.75
$B_{iso}/Å^2$	6.90	6.90	6.60	6.60
R	0.230	0.231	0.204	0.202
R_w	0.196	0.196	0.183	0.184
R(excl unobs)	0.149	0.149	0.141	0.143
R_w(excl unobs)	0.147	0.147	0.141	0.143

[a] $\theta_3 = 360n - (\theta_1 + \theta_2)$ ($n = 0$ or 1).

The measured intensities (I_o) were corrected for the Lorentz and polarization factors (L_p) by using the following equation.[8,9] The absorption effect was not corrected in this study.

$$F_o = \sqrt{\frac{I_o}{Lp}}$$

$$\frac{1}{Lp} = \frac{4\pi(1+K)\sin\theta\sqrt{\cos^2\theta - \cos^2\sigma}}{1 + K\cos^2 2\theta}$$

$$K = 1 + \cos^2 2\theta m \quad \text{and} \quad \sigma = \tan^{-1}\frac{(\zeta)}{(\xi)}$$

in which, F_o is the observed structure factor, I_o is the observed intensity, θ is the Bragg angle of the reflection, θ_m is 13.29° for the (002) reflection plane of the carbon graphite monochromator, and (ξ, ζ) are the cylindrical polar coordinates in reciprocal space.

Since the number of independently observed diffraction spots was only 24, the reflections below the observed threshold were also included in the data for the refinement calculations. The reflection with spacings longer than those of the observed ones were assumed to have half the intensity for the observational threshold. These unobserved reflection data were used only when the magnitude of the calculated structure amplitude became larger than those of the estimated structure amplitude ($|F_c| > |F_o|$) during the refinement calculations.

Molecular Model Building. The molecular model which has the 1/1 helical symmetry and the observed fiber repeating period of 16.78 Å was generated with a linked-atom description and all constant bond lengths and angles. The atomic numberings and the values of bond lengths and angles are shown in Figure 1. All hydrogen atoms were linked to the corresponding carbon atoms with a bond length of 1.08 Å and a bond angle of 120°. There are three conformational angles θ_1 (C_2–C_1–C_{20}–C_{19}), θ_2 (C_{18}–C_{17}–N_2–C_{11}), and θ_3 (C_7–N_1–C_4–C_3) in a chemical repeating unit (a). Since they were the

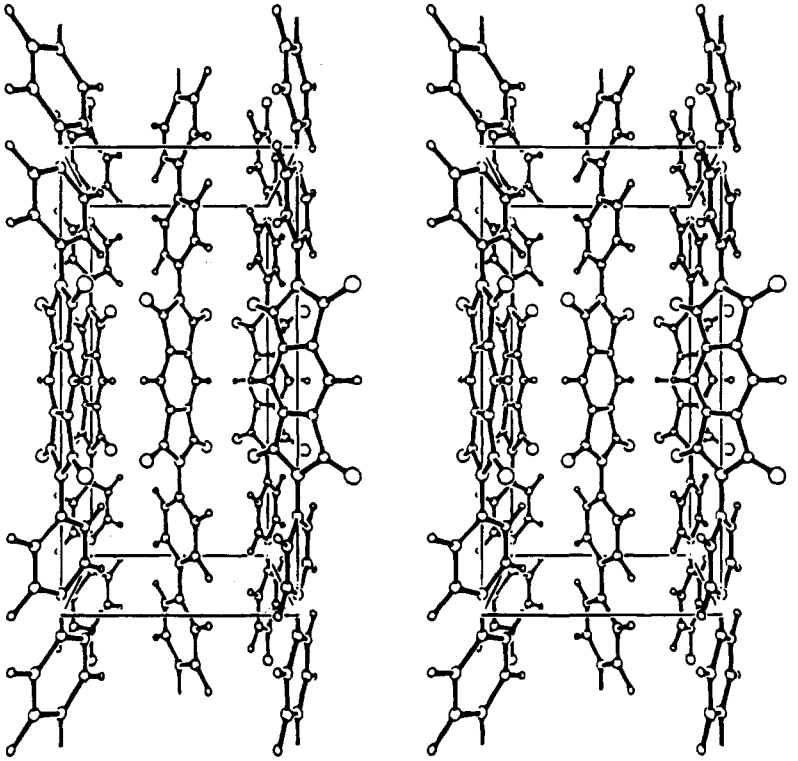

Figure 3. Stereoscopic view of PMB (ORTEP drawing[12]). The *a*-axis is horizontal, the *c*-axis is vertical, and the *b*-axis points out of the paper.

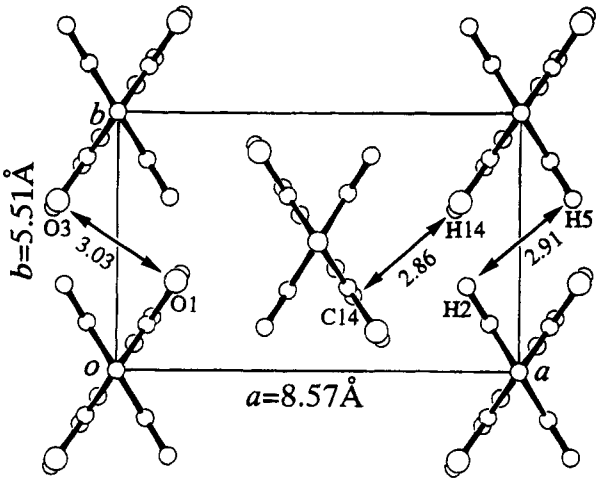

Figure 4. Packing structure of PMB viewed along the *c*(fiber)-axis. Some short contacts between neighboring molecules are shown.

angles between two para-linked phenyl moieties and between the phenyl and para-linked pyromellitimide moiety, a summation of these three angles equals 0° ($\theta_1 + \theta_2 + \theta_3 = 0°$). As a starting molecular conformation, the angles θ_1, θ_2, and θ_3 were systematically changed by 22.5° intervals starting from 0 to 157.5°. This generated a total of 64 ($=8^2$) molecular conformation models.

Packing Models and Their Refinement. To obtain appropriate packing models, the coordinates of the original atom (u, v, w) along the *a*-, *b*-, and *c*-axes and the rotational angle (μ) defined by the angle between a pyromellitimide plane and the (010) plane have to be determined. Since the (110) reflection had a very strong intensity, two chains were located at the corner $u = 0$, $v = 0$ and at the center $u = 1/2$, $v = 1/2$ of the rectangular cell projected along the *c*-axis. The chain translational parameter (w) was the fractional coordinate along the *c*-axis of the origin (N_2 atom of the corner). As shown in the following section, we performed the structure analysis for $P2_12_12$. In this space group, two chains must be arranged in the antiparallel fashion, since these chains must be related by the 2_1 symmetry perpendicular to the *c*-axis. For each model, the rotational angle (μ) of the polymer chain and the translational parameter (w) were systematically changed by 20° intervals from 0 to 160° and by 0.05 from 0 to 0.45, respectively. A total of 5760 ($=64 \times 9 \times 10$) packing models were generated. Intermolecular short contacts between nonbonded atoms and the structure amplitudes were calculated for each model. The calculated latter factors were compared to the observed ones.

At each stage of the modeling and refinement, the quantity Ω was minimized in the following least-squares fashion.[10]

$$\Omega = \sum w(|F_o| - |F_c|)^2 + s\sum \epsilon_j + \sum \lambda_h G_h$$

The first term ensures the optimum agreement between the observed (F_o) and the calculated (F_c) X-ray structure amplitudes. The weight of the reflection, w was fixed to 1.0 in this study. The second ensures the optimization of noncovalent interatomic interactions. The third imposes, by the method of Lagrange undetermined multipliers, the exact constraints we have chosen. The agreement between observed and calculated strucure amplitudes was evaluated by R and R_w, which were defined by

$$R = \frac{\sum ||F_o| - |F_c||}{\sum |F_o|} \qquad R_w = \frac{\sum (|F_o| - |F_c|)^2}{\sum F_o^2}$$

Atomic scattering factors for calculating structure factors were obtained using the method and values given in ref 11. Computations were done on the ACOS 3700/8 computer at the General Information Processing Center, Tokyo University of Agriculture and Technology.

Result and Discussion

Crystal Data. Figure 2 shows an X-ray diffraction diagram (a) of the oriented PMB specimen and its schematic illustration (b). A total of 32 (including 8 meridional reflections) observed diffraction spots was indexed by the rectangular unit cell with dimensions of $a = 8.57$, $b = 5.51$, and c (fiber axis) = 16.78 Å. The

Table 2. Fractional Atomic Coordinates of PMB

atom	x	y	z
C_1	0.000	0.000	0.044
C_2	−0.074	0.186	0.086
C_3	−0.074	0.186	0.169
C_4	0.000	0.000	0.210
C_5	0.074	−0.186	0.086
C_6	0.074	−0.186	0.169
C_7	0.075	0.176	0.345
C_8	0.044	0.103	0.428
C_9	0.088	0.208	0.500
C_{12}	−0.075	−0.176	0.345
C_{13}	−0.044	−0.103	0.428
C_{14}	−0.088	−0.208	0.500
N_1	0.000	0.000	0.298
O_1	0.147	0.346	0.319
O_3	−0.147	−0.346	0.319
H_2	−0.131	0.331	0.054
H_3	−0.131	0.331	0.201
H_5	0.131	−0.331	0.054
H_6	0.131	−0.331	0.201
H_9	0.158	0.372	0.500
H_{14}	−0.158	−0.372	0.500

unit cell was found to contain two chemical repeating units. The calculated density 1.54 g/cm^3 was in considerable agreement with the observed values (1.45 g/cm^3).

Although the number of observed reflections was not enough to determine the space group, reflections of (h00) with h odd and those of (0$k$$l$) with k odd were not observed. Since the diffraction diagram contained not so many reflections, we examined orthorhombic space groups at first. In this case, molecular symmetries, such as an inversion and a mirror symmetry, must be coincided with the crystallographic symmetry. Since the (110) reflection had a very strong intensity, two chains were located at the center and the corner. The suitable space groups satisfied with the above requirements were $P222$, $Pmm2$, $Pmmm$, $P22_12$, $P2_122$, $P2_1am$, $Pb2_1m$, $Pba2$, $Pbam$, and $P2_12_12$. In cases of the former five space groups, molecules have a 2-fold axis along the a- or b-axis or a mirror plane coincided with the ac-plane or bc-plane. Therefore the pyromellitimide and two benzene ring planes had to be at least parallel to either the a- or b-axis. After refinement against equatorial reflections, however, these five space groups were excluded because of the poor agreement between observed and calculated structure amplitudes. On the other hand, the latter five space groups correspond to the special case of $P2_12_12$ in this study where the polymer chain at the special position has the 2-fold and the inversion symmetry. Therefore, we performed the structure analysis for $P2_12_12$ in the following sections.

Molecular and Crystal Structure. In order to get appropriate packing parameters, the discrepancy factors (R and R_w) and the shortest contact between nonbonded atoms were calculated for every 5760 packing models. A total of 10 models having R values less than 0.4 and the shortest contact larger than 1.7 Å were selected and refined further against the variable parameters of θ_1, θ_2, θ_3, μ, w, a scale factor, and an overall isotropic thermal parameter (B_{iso}). As a result, three models with R values less than 0.25 and the shortest contact larger than 1.8 Å were obtained. Final parameters of these three models for $P2_12_12$ space group are summarized in Table 1. The values of conformational angles, rotational angle (μ), and translational parameter (w) for the two of them were $\theta_1 = 20.7°$, $\theta_2 = -75.9°$, $\theta_3 = 55.2°$,

Table 3. Observed (F_o) and calculated (F_c) structure amplitudes of PMB[a]

refl no.	h	k	l	F_c	F_o	refl no.	h	k	l	F_c	F_o
1	1	1	0	153.3	151.5	35	2	2	3	22.0	20.6
2	2	0	0	141.8	139.8	36	4	0	3	8.7	(10.4)
3	2	1	0	40.7	45.4	37	4	1	3	11.9	(10.9)
4	0	2	0	30.4	(8.9)	38	3	2	3	10.9	(10.9)
5	1	2	0	30.0	(9.1)	39	1	1	4	1.1	(6.7)
6	3	1	0	106.2	116.1	40	2	0	4	7.2	(6.9)
7	2	2	0	18.6	27.8	41	2	1	4	11.1	(7.9)
8	4	0	0	13.7	(10.4)	42	0	2	4	27.2	20.2
9	4	1	0	15.7	(10.8)	43	1	2	4	8.4	(9.2)
10	3	2	0	1.4	(10.9)	44	3	1	4	9.9	(9.4)
11	1	1	1	1.7	(6.7)	45	2	2	4	25.4	40.8
12	2	0	1	3.5	(6.9)	46	4	0	4	13.0	(10.4)
13	2	1	1	118.2	117.3	47	4	1	4	11.4	(10.9)
14	0	2	1	3.1	(8.9)	48	1	1	5		
15	1	2	1	10.0	(9.1)		2	0	5	19.2	31.7
16	3	1	1	10.4	(9.3)	49	2	1	5	37.9	47.5
17	2	2	1	1.1	(9.8)	50	0	2	5	22.0	33.7
18	4	0	1	9.6	(10.4)	51	1	2	5		
19	4	1	1				3	1	5	30.1	25.9
	3	2	1	62.4	70.6	52	2	2	5	6.6	(9.9)
20	1	1	2	9.2	(6.7)	53	4	0	5	22.3	(10.4)
21	2	0	2	6.7	(6.9)	54	1	1	6		
22	2	1	2	12.9	(7.9)		2	0	6	19.5	29.3
23	0	2	2	4.1	(8.9)	55	2	1	6	49.3	52.6
24	1	2	2	26.6	24.5	56	0	2	6	24.8	29.3
25	3	1	2	21.9	(9.4)		1	2	6		
26	2	2	2	14.3	(9.9)	57	3	1	6	19.9	24.4
27	4	0	2	6.7	(10.4)	58	1	1	7	2.7	(5.8)
28	4	1	2	18.0	(10.8)	59	2	0	7	3.8	(6.2)
29	3	2	2	15.9	(10.9)	60	2	1	7	3.9	(7.5)
30	1	1	3	9.1	22.5	61	0	2	7	18.4	22.6
31	2	0	3	9.9	(6.9)	62	1	1	8		
32	2	1	3	78.1	83.6		2	0	8	35.5	9.1
33	0	2	3	10.4	(8.9)						
34	1	2	3								
	3	1	3	35.9	38.8						

[a] Reflections with F_o values in parentheses are unobserved ones. These values were obtained from half of the observational threshold.

$\mu = 56.4°$, and $w = 0.296$ (model A), $\theta_1 = 159.2°$, $\theta_2 = 76.0°$, $\theta_3 = 124.9°$, $\mu = 56.4°$, and $w = 0.296$ (model A'). Their discrepancy factors were $R = 0.230$ and $R_w = 0.196$ (model A) and $R = 0.231$ and $R_w = 0.196$ (model A'). Since the sum of the corresponding dihedral angles in both models was equal to 0 or 360°, one of two models was the enantiomorph of the other, which means that these two models are essentially the same. In the case of model B, these values were $\theta_1 = -0.4°$, $\theta_2 = -65.6°$, $\theta_3 = 65.2°$, $\mu = 56.5°$, and $w = 0.301$. The discrepancy factors R and R_w were 0.204 and 0.183, respectively.

The main difference in the molecular conformation between models A and B was the dihedral angle (θ_1) of the biphenyl moiety. This was 20.7° in the model A and 0.4° in the model B. There were no significant differences in the packing parameters. The rotational angle (μ) showed almost the same values ($\mu = 56.4°$ in model A, and $\mu = 56.5°$ in model B). Adjacent pyromellitimide groups were aligned side by side at the same level along the c-axis. Because of the coplanar conformation of a biphenyl group in model B, the structure had a pseudomirror symmetry perpendicular to the c-axis. This suggested the possibility of the space group *Pbam*, as a special case of $P2_12_12$. Therefore, the structure analysis was also examined for *Pbam*. To ensure this space group symmetry, the constraining conditions of $\theta_2 + \theta_3 = 0°$, $\theta_1 = 0°$, and $w = 0.2982$ were applied and the structure was further refined against variable parameters of θ_2, θ_3, μ, B_{iso}, and a scale factor. The obtained model (model B') showed fairly good values of discrepancy factors ($R = 0.202$ and $R_w = 0.184$) and the conformational angles, $\theta_2 = -65.0°$ and $\theta_3 = 65.0°$ (Table 1). Compared with model B, model B' is definitely better, because the number of variable parameters of the latter model is less than that of the former model by 2, in spite of the almost identical R values.

In the next step, two models (A and B') must be compared. The difference of these models was the conformation of the biphenyl moiety. The dihedral angle θ_1 between the phenyl rings of the biphenyl moiety in model A was 20.7°. On the other hand, the biphenyl moiety took a coplanar conformation in model B'. The pyromellitimide plane in both models was inclined 56.5° (±0.1°) to the (010) plane. In general, the dihedral angle θ_1 between the phenyl rings was about 42° in the gas phase.[13] On the other hand, in the solid state at room temperature, two cases were reported. One is 0° and the other is around 40°. For example, the dihedral angles in the modifications of 4-hydroxybiphenyl,[14] 4,4'-bis(4-fluorobenzoyl)biphenyl,[15] and biphenyl itself[16] were almost 0°. However, these were 28.7, 35.7, and 32.2° in the structure of 4-biphenylcarboxylic acid,[17] 31.0° in 3-chlorobiphenyl-4-carbonitrile,[18] and 46° in 4-biphenylyl thioketone.[19] In the former cases, biphenyl planes stacked regularly and made a well-ordered arrangement in the crystal structures. In these letter cases, the intermolecular interaction in a well-ordered structure seems to stabilize the planar biphenyl conformation ($\theta_1 = 0°$) with the high intramolecular energy. The crystal structure of model B' showed the same type of well-ordered packing arrangement. On the other hand, the dihedral angle ($\theta_1 = 21°$) between the phenyl rings of model A deviated from both values for the coplanar type ($\theta_1 = 0°$) and the nonplanar type ($\theta_1 \approx 40°$). Furthermore, the molecular simulation techniques showed that the biphenyl moiety in this specimen was coplanar.[20] Besides the slightly better R values of model B', the above facts prompted us to take model B' as the most plausible model for this specimen. Packing structures of model B' are shown in Figures 3 and 4. The fractional atomic coordinates and the observed and calculated structure amplitudes were listed in Tables 2 and 3, respectively.

The crystal lattice of PMB contained two molecules located at the corners and the center. The molecular chain has a mirror plane perpendicular to the c-axis and glide symmetry along the a- and b-axis. The extended polymer chains were aligned side by side along the c-axis in which the pyromellitimide plane was inclined 56.6° to the (010) plane. This alignment was also found for the case of the structure of poly[(4-phenylene)-pyromellitimide].[2]

References and Notes

(1) Baklagina, Y. G.; Mileskaya, I. S.; Efanova, N. V.; Sidorovich, A. V.; Zubkou, V. A. *Vysokomol. Soedin.* **1976**, *A18*, 1235.
(2) Okuyama, K.; Sakaitani, H.; Arikawa, H. *Macromolecules* **1992**, *25*, 7261.
(3) *Polyamic Acids and Polyimides*; Michael, M. I., Zubkov, V. A., Eds.; CRC Press: Boca Raton, FL, 1993; Chapter 4.
(4) Obata, Y.; Okuyama, K. *Kobunshi Ronbunshu*, **1994**, *51*, 371.
(5) Jinda, T.; Matsuda, T.; Sakamoto, M. *Sen-i Gakkaishi* **1984**, *40*, 480.
(6) Tanaka, I.; Yao, M.; Suzuki, M.; Hikichi, K.; Matsumoto, T.; Kozasa, M.; Katayama, C. *J. Appl. Crystallogr.* **1990**, *23*, 346.
(7) Miyahara, J.; Takahashi, K.; Amemiya, Y.; Kamiya, N.; Satow, Y. *Nucl. Instrum. Methods Phys. Res.* **1986**, *A246*, 572.
(8) Cella, R. J.; Lee, B.; Hughes, R. E. *Acta Crystallogr.* **1970**, *A26*, 118.
(9) *X-Ray Structure Determination*; Stout, G. H., Jensen, L. H., Eds.; Macmillan Press: London, 1968; Chapter 7.
(10) Smith, P. J. C.; Arnott, S. *Acta Crystallogr.* **1978**, *A34*, 3.
(11) *International Tables for Crystallography*; Ibers, J. A., Hamilton, W. C., Eds.; Kynoch Press: Birmingham, England, 1974; Vol. 4, pp 71–147.
(12) Johnson, C. K. Report ORNL-5138; Oak Ridge National Laboratory: Oak Ridge, TN, 1976.
(13) Almenningen, A.; Bastiansen, O. *Skr. Kgl. Nor. Vidensk. Selsk.* **1958**, *4*, 1.
(14) Brock, C. P.; Haller, K. L. *J. Phys. Chem.* **1984**, *88*, 3570.
(15) Colquhoun, H. M.; Dudman, C. C.; Blundell, D. J.; Bunn, A.; Mackenzie, P. D.; McGrail, P. T.; Nield, E.; Rose, J. B.; Williams, D. J. *Macromolecules* **1993**, *26*, 107.
(16) Charbonneau, G. P.; Delugeard, Y. *Acta Crystallogr.* **1977**, *B33*, 1586.
(17) Brock, C. P.; Blackburn, J. R.; Haller, K. *Acta Crystallogr.* **1984**, *B40*, 493.
(18) Sutherland, H. H.; Rawas, A. *Acta Crystallogr.* **1984**, *C40*, 830.
(19) Arjunnan, P.; Ramamurthy, V.; Venkatesan, K. *Acta Crystallogr.* **1984**, *C40*, 556.
(20) Kitano, Y.; Usami, I.; Obata, Y.; Okuyama, K.; Jinda, T. *Polymer*, in press.

MA9412290